Cell-biologic and functional analysis of five new Aquaporin-2 missense mutations that cause recessive Nephrogenic Diabetes Insipidus

Marr N, Bichet DG, Hoefs S, Savelkoul PJM, Koenings IBM, de Mattia F, Graat MPJ, Arthus MF, Lonergan M, Fujiwara M, Knoers NVAM, Landau D, Balfe J, Oksche A, Rosenthal W, **Müller D**, van Os CH, Deen PMT

J Am Soc Nephrol 2002; 13: 2267-2277

J Am Soc Nephrol 13: 2267–2277, 2002

Cell-Biologic and Functional Analyses of Five New *Aquaporin-2* Missense Mutations that Cause Recessive Nephrogenic Diabetes Insipidus

NANNETTE MARR,* DANIEL G. BICHET,† SUSAN HOEFS,* PAUL J. M. SAVELKOUL,* IRENE B. M. KONINGS,* FABRIZIO DE MATTIA,* MICHAEL P. J. GRAAT,* MARIE-FRANÇOISE ARTHUS,† MICHELE LONERGAN,† T. MARY FUJIWARA,‡ NINE V. A. M. KNOERS,§ DANIEL LANDAU,¶ WILLIAM J. BALFE,# ALEXANDER OKSCHE,‖ WALTER ROSENTHAL,‖ DOMINIK MÜLLER,* CAREL H. VAN OS,* and PETER M. T. DEEN*

*Departments of *Cell Physiology and §Human Genetics, UMC St. Radboud, Nijmegen, The Netherlands; †Department of Medicine, University of Montreal and Centre de Recherches, Hôpital du Sacre-Coeur de Montreal, Montreal, Quebec, Canada; ‡Departments of Human Genetics and Medicine, McGill University and Research Institute of the McGill University Health Centre, Montreal, Canada; ¶Department of Pediatrics, Soroka Medical Center, Beer Sheva, Israel; #Department of Pediatrics, The Hospital for Sick Children, University of Toronto, Toronto, Canada; and ‖Forschungsinstitut für Molekulare Pharmakologie, Berlin, Germany.*

Abstract. Mutations in the *Aquaporin-2* gene, which encodes a renal water channel, have been shown to cause autosomal nephrogenic diabetes insipidus (NDI), a disease in which the kidney is unable to concentrate urine in response to vasopressin. Most AQP2 missense mutants in recessive NDI are retained in the endoplasmic reticulum (ER), but AQP2-T125M and AQP2-G175R were reported to be nonfunctional channels unimpaired in their routing to the plasma membrane. In five families, seven novel *AQP2* gene mutations were identified and their cell-biologic basis for causing recessive NDI was analyzed. The patients in four families were homozygous for mutations, encoding AQP2-L28P, AQP2-A47V, AQP2-V71M, or AQP2-P185A. Expression in oocytes revealed that all these mutants, and also AQP2-T125M and AQP2-G175R, conferred a reduced water permeability compared with wt-AQP2, which was due to ER retardation. The patient in the fifth family had a G>A nucleotide substitution in the splice donor site of one allele that results in an out-of-frame protein. The other allele has a nucleotide deletion (c652delC) and a missense mutation (V194I). The routing and function of AQP2-V194I in oocytes was not different from wt-AQP2; it was therefore concluded that c652delC, which leads to an out-of-frame protein, is the NDI-causing mutation of the second allele. This study indicates that misfolding and ER retention is the main, and possibly only, cell-biologic basis for recessive NDI caused by missense AQP2 proteins. In addition, the reduced single channel water permeability of AQP2-A47V (40%) and AQP2-T125M (25%) might become of therapeutic value when chemical chaperones can be found that restore their routing to the plasma membrane.

The aquaporin-2 (AQP2) water channel plays an important role in reabsorption of water in the kidney collecting duct and consequently in concentrating urine (1). Binding of arginine vasopressin (AVP) to its V2 receptor (AVPR2) at the basolateral side of principal cells of collecting ducts leads to an increase of intracellular cAMP levels, resulting in phosphorylation of AQP2 and possibly other proteins, by protein kinase A and subsequent redistribution of AQP2 from subapical storage vesicles to the apical plasma membrane. Driven by the interstitial hypertonicity, water reabsorption and urine concentration is thereby initiated. This process is reversed after dissociation of AVP from its receptor (2,3).

Several mutations in the *AVPR2* and *AQP2* genes have been reported to cause congenital nephrogenic diabetes insipidus (NDI), a disease in which the kidney is unable to concentrate urine in response to AVP. Mutations in the *AVPR2* gene result in NDI that is inherited as an X-linked recessive trait, whereas mutations in the *AQP2* gene cause NDI that is inherited as either an autosomal recessive or a dominant trait (1,4–6,7). Expression studies in oocytes showed that an AQP2 mutant in dominant NDI, AQP2-E258K, was a functional water channel but was retained in the region of the Golgi complex (7). In coexpression studies with wild-type (wt) AQP2, a dominant-negative effect was observed, which was caused by impaired routing of wt-AQP2 to the plasma membrane because of het-

Received October 18, 2001. Accepted June 3, 2002.
Correspondence to Dr. Peter M. T. Deen, 162, Department of Cell Physiology, NCMLS, UMC St Radboud, PO Box 9101, 6500 HB Nijmegen, The Netherlands. Phone: 31-24-361-7347; Fax: 31-24-3616430; E-mail: peterd@sci.kun.nl
1046-6673/1309-2267
Journal of the American Society of Nephrology
Copyright © 2002 by the American Society of Nephrology
DOI: 10.1097/01.ASN.0000027355.41663.14

erotetramerization with AQP2-E258K (8). Recently, four other AQP2 mutants, all with nucleotide deletions in the coding region of the C-terminus of AQP2, were reported to cause dominant NDI (9,10). Similar to AQP2-E258K, expression of these AQP2 mutants in oocytes revealed that they were functional water channels, which conferred their dominant-negative effect by heteroligomerization with wt-AQP2 and mistargeting of the wt-mutant complex to another subcellular organelle than the plasma membrane.

Most mutations identified in the *AQP2* gene, however, cause NDI that is inherited as an autosomal recessive trait. On the basis of the cell-biologic outcome for plasma membrane proteins, genotypes have been assigned to five different classes (11,12). Functional analyses of numerous mutants revealed that more than 50% of mutations identified in inherited diseases are class II mutations. With class II mutations, the translation of the protein is complete, but the abnormal protein fails to be exported from the endoplasmic reticulum (ER; for review see reference 13). Retention in the ER is usually followed by degradation of the protein (14); consequently, little or no protein reaches its final destination. Similarly, expression in oocytes of missense AQP2 mutants in recessive NDI revealed that most were impaired in their export from the ER (15–18).

In contrast to these class II *AQP2* mutations, Goji *et al.* described two mutations in recessive NDI that would fall into class IV, because the corresponding AQP2 mutants (AQP2-T125M and AQP2-G175R) were reported to be nonfunctional channels that were not impaired in their routing to the plasma membrane (19). This suggested that there are at least two mechanisms by which *AQP2* missense mutations can cause recessive NDI.

In this article, five NDI families are described in whom seven new *AQP2* mutations were identified, of which five were missense mutations. To determine their involvement in recessive NDI and the cell-biologic mechanism underlying NDI in these families, the encoded AQP2 mutants were tested for their routing and function in *Xenopus* oocytes and, to some extent, in polarized MDCK cells. Also included in this study were the two class IV mutations (T125M and G175R) that were reported to encode nonfunctional water channels.

Materials and Methods

Patients

Patient characteristics are illustrated in Figure 1. The index patient of family 1 was administered to the hospital at the age of 1 mo because of vomiting and failure to thrive. The female patient was the second child of consanguineous parents and had a healthy brother. Blood and urine analyses revealed hypernatremia (160 mmol/L) and low urine osmolality (89 mosmol/kg H_2O), respectively. Uosm did not increase after administration of dDAVP, indicating that the child suffered from NDI. At the age of 6 yr, she is still small and has mild hydronephrosis. Both patients from family 2 presented in early infancy with fever, vomiting, polyuria, polydipsia, dehydration, and failure to thrive. On biochemical analysis, both showed hypernatremia (152 and 153 mmol/L) and low urinary osmolality (230 and 224 mosm/kg H_2O). During an oral fluid deprivation trial with consecutive dDAVP administration (40 μg intranasally), urinary osmolality did not increase (189 and 185 mosmol/kg H_2O). Family 3 is a consanguineous family of Pakistani origin with two affected girls. The parents are most closely related as first cousins. Both patients presented with polydipsia, severe polyuria and low urinary osmolality (96 and 112 mosmol/kg H_2O), which did not increase after dDAVP administration (91 and 123 mosmol/kg H_2O). The patient from family 4 presented 5 d after birth with fever and bloody feces. She is the first child of parents of German origin who are related as first cousins, once removed. Clinical testing revealed hypernatremia (150 mmol/L) and a urinary osmolality of 84 to 150 mosm/kg H_2O, which did not increase with dDAVP administration (150 mosm/kg H_2O). The patient from family 5 presented with vomiting within the first week of life, which became severe in the following 2 wk. Biochemical analysis at the age of 6 wk revealed hypernatremia (155 to 160 mmol/L) and an elevated plasma osmolality (324 mosmol/kg). The urinary osmolality of 80 mosmol/kg H_2O did not increase after intramuscular or subcutaneous administration of dDAVP. Isolation of genomic DNAs, amplification of the *AVPR2* and *AQP2* coding regions, and sequence analyses were done as described (1,20,21).

Generation of AQP2 Mutant Expression Constructs

With a three-steps PCR reaction or quick-change site-directed mutagenesis kit (T125M; Stratagene, Heidelberg, Germany), each mutation carried by NDI patients was introduced into the human *AQP2* cDNA sequence. Primers used were CGTCTTC-TTTGGC*CCCGGG*TCTGCCCTCAACTGG for L28P, CCCT-CTGTG*CTGCAG*ATTGCCATGGTGTTTGGCTTGG for A47V, AGCGGGGCCCACATCAA*CCCGG*CCATGACTGTGGCCTGC for V71M, GCTCTGAGCAACAGCATGACGGCCGGCCAGGCGG for T125M, GGTGTAATGGATC*CGAAGG*AGGTGGCC for G175R, GCTCTATGAATGCTG*CCCGG*TCCCTGGCTCCAGC for P185A, and GCTCCCTGGCTC*CGGCTG*TCATCACTGGCAAATTTG for V194I, with which restriction sites were introduced for *Sma*I (L28P), *Pst*I (A47V), or *Nci*I (V71M, P185A) or were deleted for *Sty*I (G175R) or *Pvu*II (V194I). After cutting these fragments with *Bgl*II/*Apa*I (L28P), *Nco*I/*Sma*I (A47V), *Apa*I/*Bam*HI (V71M, G175R), *Apa*I/*Sma*I (T125M), or *Bam*HI/*Kpn*I (P185A, V194I), the mutation-containing fragments were isolated and cloned into the corresponding sites of the oocytes expression construct pT_7T_s-*AQP2* (1).

For expression in MDCK cells, wt-AQP2, AQP2-R187C, and AQP2-T125M were N-terminally tagged with the green fluorescent protein (GFP). For the generation of GFP-tagged wt-AQP2 (G-AQP2), a 900-bp *Nsp*I-blunted/*Sal*I fragment of pBS-*AQP2* (1), which contained the complete wt-AQP2 coding sequence, was cloned into the *Hin*dIII-blunted/*Sal*I sites of pEGFP-C1 (Clontech, Palo Alto, CA), resulting in pEGFP-*AQP2*. To facilitate cloning of *AQP2* mutants in pEGFP-C1, the *Apa*I and *Kpn*I sites were removed by digestion with *Sma*I and *Kpn*I, after which the vector was blunted with T4 DNA polymerase and re-ligated. An 865-bp *Bgl*II/*Sal*I fragment of pEGFP-*AQP2* was subsequently cloned into the corresponding sites of this pEGFP-ΔAK vector to generate pEGFP-ΔAK-*AQP2*. To generate the fusion constructs encoding GFP-AQP2-R187C (G-AQP2-R187C) and GFP-AQP2-T125M (G-AQP2-T125M), 611-bp *Apa*I/*Kpn*I fragments, encoding *AQP2* segments containing the mutations, were isolated from pTsT7-*AQP2*-R187C and pTsT7-*AQP2*-T125M, respectively, and cloned into the corresponding sites of pEGFP-ΔAK-*AQP2*. Sequence analysis of selected clones confirmed that only the desired mutations were introduced.

Generation of cRNAs

Expression constructs pT_7T_s-*AQP2*, pT_7T_s-*AQP2*-L28P, pT_7T_s-*AQP2*-A47V, pT_7T_s-*AQP2*-V71M, pT_7T_s-*AQP2*-T125M, pT_7T_s-

AQP2-G175R, pT_7T_s-*AQP2*-P185A, and pT_7T_s-*AQP2*-V194I were linearized with *SalI*, after which g-capped cRNA transcripts were synthesized *in vitro* using T7 RNA polymerase according to Promega's Protocols and Principle guide (1991), except that 1 mM final concentration of nucleotide triphosphates and m7G(5')ppp(5')G were used. The cRNAs were phenol extracted, precipitated and dissolved in di-ethylpyrocarbonate–treated water. The integrity was checked by agarose gel electrophoresis, and the concentrations were determined with a spectrophotometer.

Water Permeability Measurements

Stage V and VI oocytes were isolated from *Xenopus laevis* after defolliculation with 2 mg/ml collagenase A (Boehringer Mannheim, Mannheim, Germany) and stored at 18°C in modified Barth solution (MBS: 88 mM NaCl, 1 mM KCl, 2.4 mM $NaHCO_3$, 10 mM HEPES [pH 7.5], 0.82 mM $MgSO_4$, 0.33 mM $Ca(NO_3)_2$, 0.41 mM $CaCl_2$) supplemented with 25 μg/ml gentamicin. The oocytes were injected with the indicated amounts of cRNAs coding for wt or mutant AQP2 proteins. Three days after injection, the vitelline membranes were removed and the water permeability (P_f in μm/s) was measured using a standard swelling assay (1). Oocyte swelling was performed at 22°C after the transfer from 200 mosM to 20 mosM.

Isolation of Total Membranes and Plasma Membranes

To isolate total membranes, 12 oocytes were homogenized in 250 μl of homogenization buffer A (HbA: 20 mM Tris [pH 7.4], 5 mM $MgCl_2$, 5 mM NaH_2PO_4, 1 mM EDTA, 80 mM sucrose, 1 mM phenylmethylsulfonyl fluoride, 5 μg/ml leupeptin and pepstatin) and centrifuged at 200 *g* at 4°C for 10 min to remove the yolk proteins. The membranes were isolated by centrifugation at 4°C at 14,000 *g* for 20 min.

Plasma membranes were isolated as described (22). Briefly, 12 oocytes were coated with 1% silica in modified MES-buffered saline for silica (MBSS: 20 mM MES, 80 mM NaCl, pH 6.0), washed twice with MBSS buffer, and incubated in 0.1% polyacrylic acid in MBSS. In both incubations, oocytes were rotated slowly for 30 min at 4°C. After two times washing with MBS, the oocytes were homogenized in HbA. After five washing steps with slow centrifugation (3×14 *g*; 1×24 *g*; 1×390 *g*) at 4°C for 30 s, plasma membranes were pelleted by centrifugation at 14,000 *g* for 20 min.

Immunoblotting

Protein samples were denatured by incubation for 30 min at 37°C in Laemmli buffer, subjected to electrophoresis on a 12% SDS-polyacrylamide gel and transferred onto PVDF membranes (Millipore Corporation, Bradford, MA) by standard procedures. Next, the blots were incubated with 1:3000 diluted affinity-purified AQP2: 257 to 271 rabbit antibodies, raised against the 15 C-terminal amino acids of rat AQP2 (15) in TBST-buffer (20 mM Tris, 140 mM NaCl, 0.1%Tween, pH 7.6) supplemented with 1% nonfat dried milk. As a secondary antibody, a 1:5000 dilution of goat α-rabbit IgG (Sigma, St Louis, MO) coupled to horseradish peroxidase was used. Finally, AQP2 proteins were visualized using enhanced chemiluminescence (Pierce, Rockford, IL). Digestion of proteins with N-glycosidase F (Boehringer Mannheim, Mannheim, Germany) was done according to the manufacturer's protocol.

Determination of the Relative Single Channel Water Permeabilities of AQP2 Mutants

To determine the functionality of AQP2 mutants in relation to wt-AQP2, all immunoblot signals of AQP2 proteins in the plasma membrane of oocytes were semi-quantified by densitometric scanning and comparison with the signals of a twofold dilution series of wt-AQP2, which was blotted in parallel. In each experiment, the different amounts of wt-AQP2 expressed in the plasma membrane fraction of oocytes and the corresponding P_f values were fitted to the exponential function $y = a(1-\exp(-bx)) + c$, where y is P_f and x is the amount of protein in arbitrary units. The amount of wt-AQP2 that would be necessary to obtain the P_f value observed for the mutants was calculated from the equation. The ratio of the amount of wt-AQP2 and mutant AQP2 for the P_f that had been obtained for the mutant indicates the single channel water permeability of the mutant relative to wt-AQP2 in percentage. Statistical significance was determined using the *t* test.

Immunocytochemistry on Oocytes

Two days after injection of oocytes with 10 ng of mutant AQP2 cRNAs or 1 ng of wt-AQP2 cRNA, vitelline membranes were removed and oocytes were incubated for 1 h in 1% wt/vol paraformaldehyde-lysine periodate fixative (23), dehydrated, embedded in paraffin, and sectioned. Potential sites for nonspecific antibody binding were blocked with 10% goat serum in PBS. Sections were incubated O/N with a 1:100 dilution of rabbit 5 α-AQP2 antibodies. After washing three times for 10 min in TBS, sections were incubated for 1 h with a 1:100 dilution of Alexa594-conjugated α-rabbit antibodies (Molecular Probes, Pitchford, Eugene). The sections were again washed three times for 10 min in TBS, dehydrated in methanol, and mounted in vectashield (Vector Laboratories, Berlingame, CA). AQP2 proteins were visualized using confocal laser scanning microscopy (CLSM; Bio-Rad MRC-1000).

MDCK Cells

Polarized Madin-Darby Canine Kidney (MDCK) type I cells (24) were cultured as described (25). To obtain expression in MDCK cells, cell clones stably expressing G-AQP2 and G-AQP2-R187C were generated and selected as described (25). For expression of G-AQP2-T125M, cells were transiently transfected with LipofectAmine according to the manufacturer's protocol (Invitrogen, Breda, The Netherlands). After growth to confluence, the cells were fixed and the AQP2 proteins were visualized by CLSM analysis as described (26).

Results

Analysis of the Patients

In families 1 to 4, affected female individuals from consanguineous parents suggested that NDI was most likely inherited as an autosomal recessive trait (Figure 1). In families 3 and 4, the NDI patients inherited identical *AQP2* gene alleles, which supported this assumption. Family 5 presented with one affected boy; therefore, a mutation in the *AVPR2* gene could not be excluded. However, sequence analysis of genomic DNA of the patient revealed no mutation in the coding or exon-flanking sequences of the *AVPR2* gene. Therefore, the *AQP2* gene of patients in these five families was analyzed. As anticipated, patients from family 1 to 4 were homozygous for an *AQP2* mutation, namely c83T>C, c140C>T, c211G>A, or c553C>G, which encoded L28P, A47V, V71M, or P185A AQP2 missense proteins, respectively (Figure 2). In family 5, the patient was a compound heterozygote for a mutation in the splice donor site of exon3/intron3 (c606+1G>A) in one allele, and a nucleotide substitution (c580G>A) combined with a

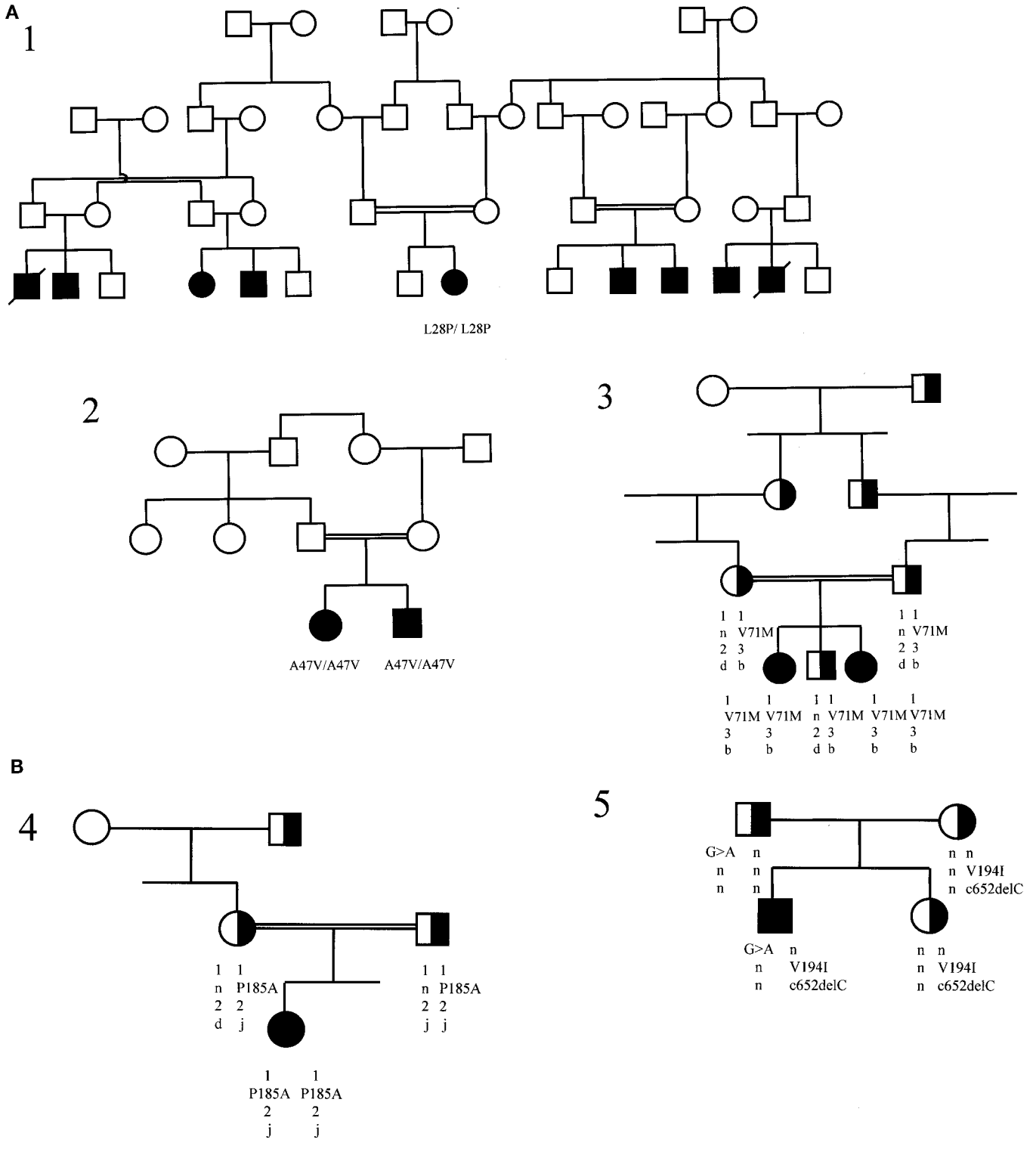

Figure 1. Segregation of nephrogenic diabetes insipidus (NDI) and Aquaporin-2 (AQP2) mutations in the studied families. For the five families studied (numbered 1 through 5), carriers (half-filled symbols), unaffected (open symbols) and affected individuals (filled symbols), and males (squares) and females (circles) are indicated. For families 3 and 4, the haplotype in chromosome region 12q13 is shown; the marker order is centromere-AFM259vf9-*AQP2*-D12S131-AFMb007yg5-telomere (52) (alleles of the dinucleotide markers are indicated by numbers or letters; for *AQP2*, the mutations or normal allele (n) are shown). For family 5, the intron 3 splice donor site mutation (G>A), V194I mutation, and exon 4 nucleotide deletion (c652delC) are indicated.

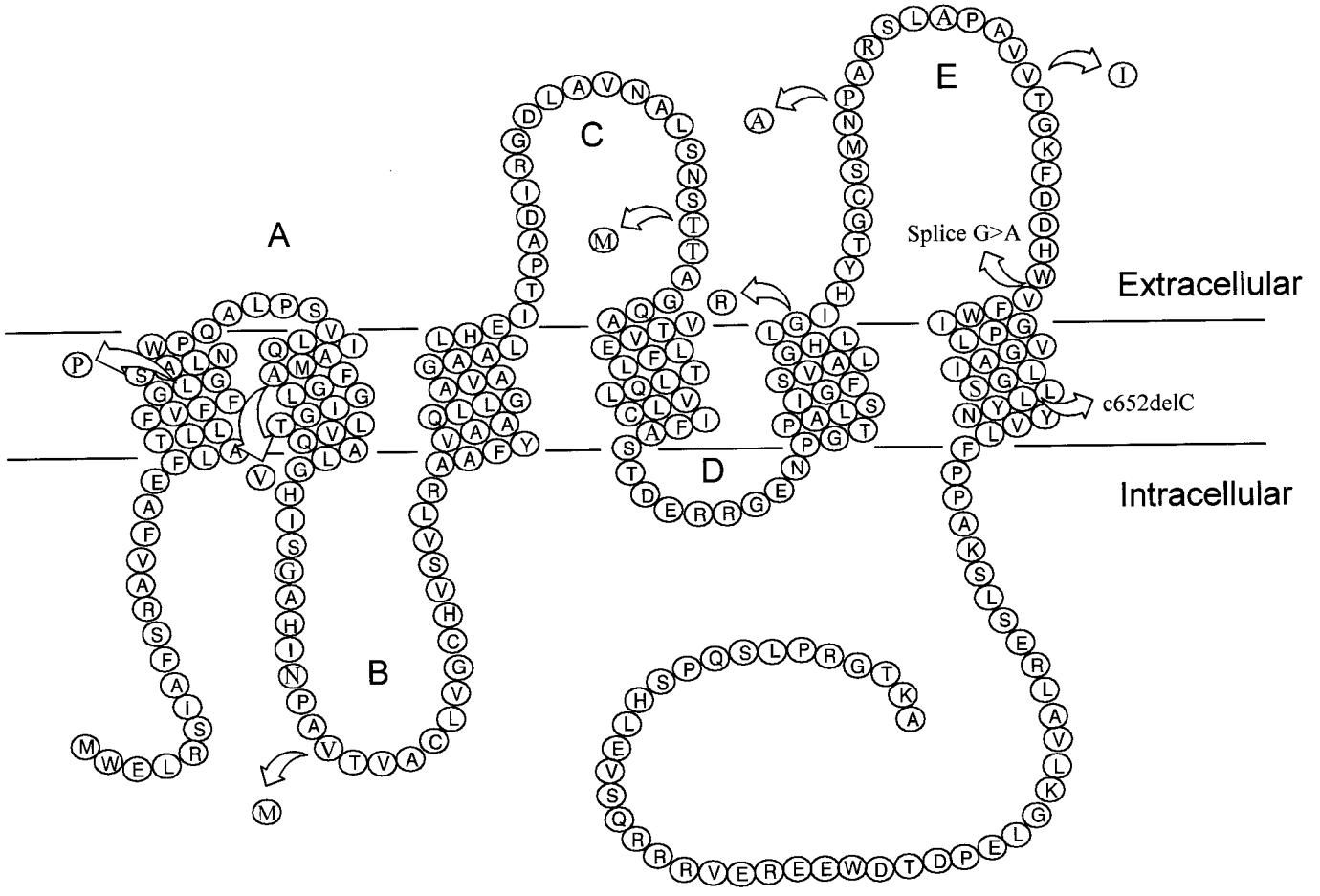

Figure 2. The localization of the mutations in AQP2. The AQP2 protein is predicted to consist of six transmembrane domains connected by loops A through E with the N and C-termini located intracellularly. In the proposed AQP2 topology, the amino acids are represented as circles and labeled with the standard single-letter designations. The missense mutations (encircled letters), splice site mutation (splice G>A), and nucleotide deletion (c652delC) as identified in the NDI patients are indicated.

nucleotide deletion (c652delC) in the other allele, which were inherited from the father and mother, respectively. The c580G>A mutation codes for a V194I mutation in AQP2.

Functional Analysis of Encoded AQP2 Missense Mutants in NDI

To determine whether the identified missense mutations could be causal for NDI, each mutation was introduced into the *AQP2* cDNA sequence, cloned into an oocyte expression vector and transcribed. In addition, two other mutants (AQP2-T125M and AQP2-G175R [Figure 2]) were included, because these mutants were suggested to be nonfunctional channels unimpaired in their routing to the plasma membrane (19). Although low expression levels already reveal whether AQP2 mutants are misfolded, high expression levels also enable us to determine whether such mutants are functional water channels, because at these levels a considerable amount of the mutants is often expressed in the plasma membrane (27,28). Therefore, oocytes were injected with 10 ng of cRNAs coding for AQP2 mutants, along with a concentration series of wt-AQP2 cRNA (0.3, 0.6, 1.2, and 2.4 ng). An exception was AQP2-V194I, of which 0.5 ng of cRNA was injected, because preliminary experiments indicated that this mutant conferred high water permeability (not shown). Three days later, water transport analysis revealed that the P_fs of oocytes expressing wt-AQP2 or the mutants AQP2-A47V, AQP2-T125M, or AQP2-V194I were significantly higher than that of control oocytes, whereas the P_fs of oocytes expressing AQP2-L28P, AQP2-V71M, AQP2-G175R, or AQP2-P185A were not different from controls (Figure 3).

To check for expression levels, total membranes and plasma membranes were isolated from these oocytes and subjected to immunoblotting for AQP2. Wt-AQP2 and all AQP2 mutants were expressed in the total membrane and plasma membrane fractions (Figure 4, panels A and B, respectively). For the AQP2 mutants AQP2-L28P, AQP2-A47V, AQP2-V71M, AQP2-G175R, and AQP2-P185A, the characteristic unglycosylated 29-kD and high-mannose glycosylated 32-kD AQP2 forms were present, whereas only a 29-kD band was detected for wt-AQP2, AQP2-T125M, and AQP2-V194I. As reported in reference 28, a decreased ratio of plasma membrane *versus* total membrane expression for an AQP2 mutant compared with

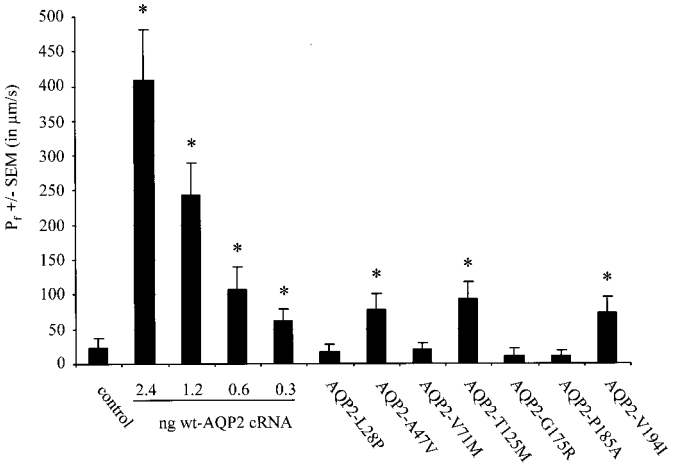

Figure 3. Osmotic water permeabilities of oocytes expressing AQP2 proteins. Three days after injection of the indicated amounts of wt-AQP2 cRNA, 0.5 ng of AQP2-V194I cRNA, or 10 ng cRNA encoding the other AQP2 mutants in recessive NDI, oocytes were subjected to a standard swelling assay. Non-injected oocytes were used as a control. Mean water permeabilities (P_f) and SEM of 12 oocytes are shown. An asterisk indicates a significant ($P < 0.01$) increase in P_f above that of control oocytes.

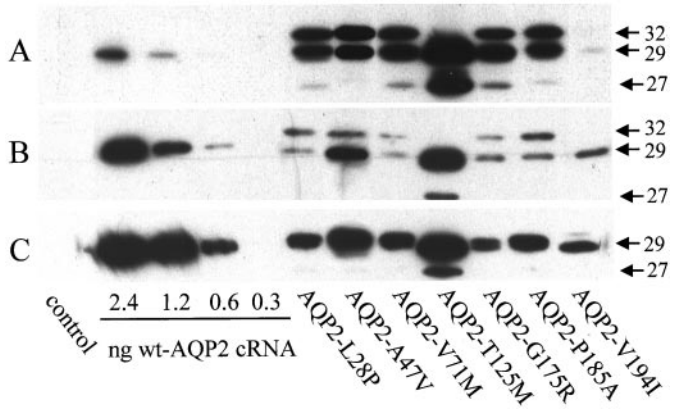

Figure 4. Immunoblot analysis of AQP2 proteins expressed in oocytes. From 12 oocytes injected as described in the legend of Figure 3, total membranes (A) or plasma membranes (B and C) were isolated. To semi-quantify the amount of AQP2 in the plasma membranes, oocyte equivalents of plasma membrane fractions were treated with N-glycosidase F before immunoblot analysis (C). Oocyte equivalents of 0.5 (A), 2 (B), or 1 (C) were immunoblotted for AQP2. The masses of unglycosylated AQP2 (29 kD), high-mannose glycosylated AQP2 (32 kD), and the degradation product of AQP2 (27 kDa) are indicated.

that of wt-AQP2 indicates that the mutant protein is retained within the cell. As can be seen in Figure 4, each AQP2 mutant showed a stronger total membrane than plasma membrane signal when compared with those signals for wt-AQP2, except for AQP2-V194I (compare lanes A and B for wt and mutant AQP2 proteins). These data indicated that all AQP2 mutants, except AQP2-V194I, were retarded in their routing to the plasma membrane. Other immunoblots and P_f measurements of oocytes injected with a concentration series of wt-AQP2 and AQP2-V194I cRNAs revealed that the routing and function of AQP2-V194I were not different from those of wt-AQP2 (not shown).

Interestingly, an AQP2 degradation product of about 27 kD was observed in the TM lanes of most AQP2 mutants, which was most prominent for AQP2-T125M (Figure 4A). Because different levels of cRNA of wt-AQP2 and AQP2 mutants were injected in these experiments, it was not clear whether this degradation product would also be found for wt-AQP2. Oocytes were therefore injected with 1-, 3-, and 10-ng cRNA amounts encoding wt-AQP2 or AQP2-T125M. Immunoblot analysis of total membranes of these oocytes revealed that this 27-kD band is indeed also found for wt-AQP2, but only at high expression levels (Figure 5). At these levels (Figure 5) but not at low expression levels (Figure 4), also some complex-glycosylated AQP2 (40 to 45 kD) is detected for wt-AQP2–expressing oocytes. As noted before (15), this might be due to a different repertoire of proteins involved in glycosylation in oocytes, because our antibodies easily detect complex-glycosylated AQP2 in renal samples (29).

Relative Water Permeabilities of Wild-Type and Mutant AQP2 Proteins

To determine the relative amounts of AQP2 in the plasma membrane, oocyte equivalents of plasma membranes were digested with N-glycosidase F to remove the sugar moieties and immunoblotted for AQP2 (Figure 4C). The amount of all mutants present in the plasma membrane fractions was consistently between the lowest and highest amounts of wt-AQP2 expressed in the plasma membranes. Comparison of the measured P_f values with the plasma membrane expression levels allowed the determination of the channel permeabilities of AQP2 mutants relative to that of wt-AQP2 (Figure 6). Previous experiments have shown that the amounts injected of wt-AQP2 are within a logarithmic phase (28); a single exponential function was therefore fitted to the P_f values and amounts of the wt-AQP2 concentration series. Subsequently, the ratio of the amounts of wt-AQP2 and AQP2 mutant conferring the partic-

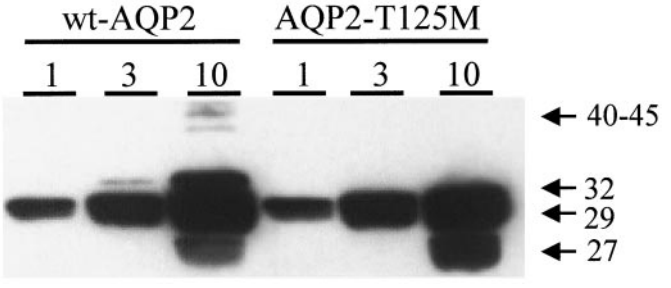

Figure 5. Forms of wt-AQP2 and AQP2-T125M at different expression levels. From 12 oocytes injected with 1, 3, or 10 ng of cRNA coding for wt-AQP2 or AQP2-T125M, total membranes were isolated. Of each injection, a one oocyte equivalent was immunoblotted for AQP2. Unglycosylated AQP2 (29 kD), high-mannose glycosylated AQP2 (32 kD), and the degradation product of AQP2 (27 kD) are indicated.

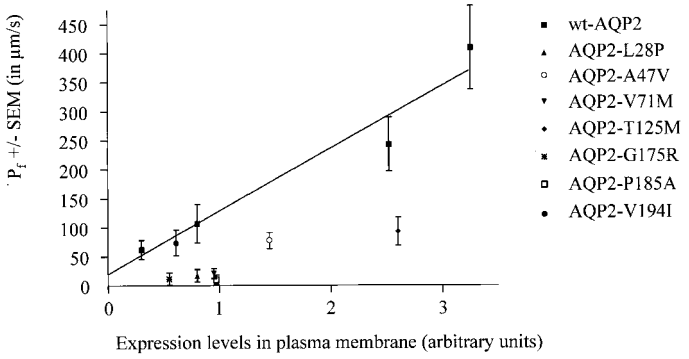

Figure 6. Functionality of AQP2 mutants. To determine the relative single channel permeability of AQP2 mutants in recessive NDI, the water permeabilities ($P_f \pm$ SEM in μm/sec) obtained for oocytes expressing wt or mutant AQP2 proteins were related to their amounts detected in the plasma membrane. The wt-AQP2 data were fitted to an exponential function (see Materials and Methods). One representative experiment is shown ($n = 12$ oocytes).

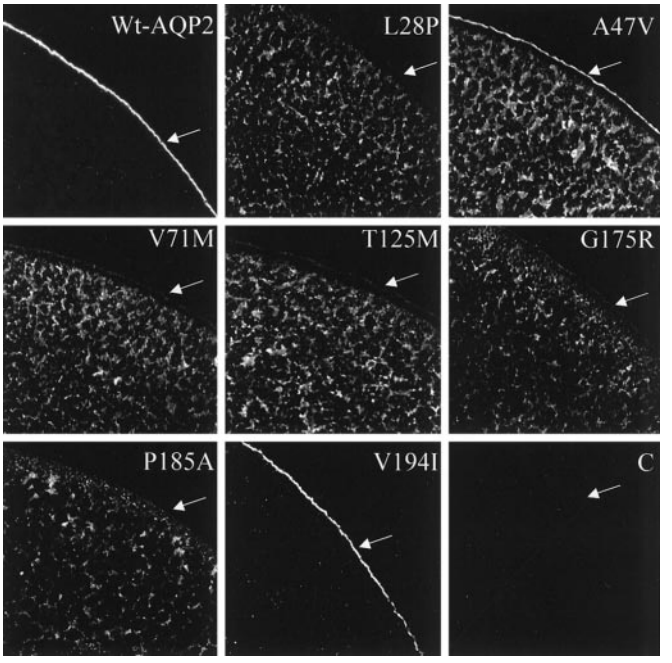

Figure 7. Localization of the AQP2 mutants in oocytes. Non-injected oocytes (C), oocytes injected with 1 ng of cRNA coding for wt-AQP2 or 10 ng of AQP2-L28P, -A47V, -V71M, -T125M, -G175R, -P185A, or -V194I were fixed in paraformaldehyde and embedded in paraffin. Sections were incubated with rabbit α-AQP2 antibodies followed by Alexa594-conjugated α-rabbit antibodies. AQP2 proteins were visualized using confocal laser scanning microscopy. The plasma membrane is indicated by an arrow.

ular P_f of the mutant AQP2 was calculated. From four such independent experiments, it was concluded that AQP2-L28P, AQP2-V71M, AQP2-G175R, and AQP2-P185A were nonfunctional water channels. In contrast, AQP2-T125M and AQP2-A47V retained about 25% and 40% of the single channel water permeability of wt-AQP2, respectively, whereas the water permeability conferred by AQP2-V194I was similar to that of wt-AQP2.

Subcellular Localization in Oocytes and MDCK Cells

To determine the subcellular expression pattern, oocytes expressing wt-AQP2 or AQP2 mutants were subjected to immunocytochemistry (Figure 7). Confocal laser scanning analysis of stained sections of these oocytes revealed a dispersed staining for AQP2-L28P, AQP2-A47V, AQP2-V71M, AQP2-T125M, AQP2-G175R, and AQP2-P185A. In addition, some plasma membrane staining was observed for oocytes expressing AQP2-A47V, AQP2-V71M, AQP2-T125M, and AQP2-G175R. In contrast, wt-AQP2 and AQP2-V194I only showed strong plasma membrane expression, while non-injected oocytes essentially revealed no labeling.

Although AQP2-T125M expression in oocytes revealed a similar distribution as the other AQP2 mutants in recessive NDI, the inability to determine whether AQP2-T125M is retained in the ER by the appearance of a 32-kD high-mannose glycosylated band in immunoblotting (Figure 4) urged us to investigate the expression of this mutant in polarized MDCK cells. Therefore, MDCK cells were transfected with constructs coding for wt-AQP2, AQP2-R187C, and AQP2-T125M coupled to GFP to facilitate detection. Immunocytochemistry and subsequent confocal laser scanning microscopy of cells transfected with these constructs revealed that GFP-AQP2 was predominantly expressed in the apical plasma membrane (Figure 8). In contrast, AQP2-R187C and AQP2-T125M showed a similar dispersed staining throughout the cell.

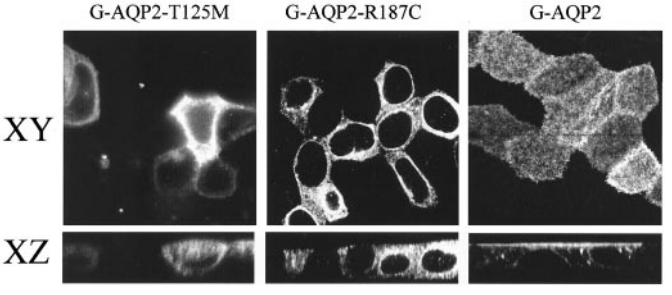

Figure 8. Localization of the AQP2-T125M in MDCK cells. MDCK cells were transfected with expression constructs encoding GFP-tagged wt-AQP2 (G-AQP2), AQP2-T125M (G-AQP2-T125M), or AQP2-R187C (G-AQP2-R187C) and grown to confluence on semipermeable filters. Following fixation and embedding in VectaShield, XY and XZ images of the localization of the AQP2 proteins were made using confocal laser scanning microscopy.

Discussion

Trafficking and Glycosylation Forms of AQP2

AQP2, like other glycosylated membrane proteins, is synthesized in the ER, where it is folded and assembled into a homotetramer. In addition, in this organelle, high-mannose sugar moieties are attached to Asn123 of AQP2, which is part of a canonical N-glycosylation consensus site (N_{123}-X-T_{125}; Figure 2). *En route* to the plasma membrane, the high-mannose

sugar groups are removed in the Golgi complex, after which these AQP2 molecules are complex glycosylated. In line with other AQPs (30,31) but in contrast to most glycosylated proteins, only one or two monomers within an AQP2 tetramer are glycosylated (32). The mass of complex glycosylated AQP2 ranges from 40 to 45 kD; these AQP2 forms are therefore only detected on immunoblots when high amounts are loaded.

Proteins that are not properly folded in the ER are thought to have extended interaction times with the ER folding proteins, named molecular chaperones (33). As such, misfolded AQP2 mutants are usually detected as high-mannose glycosylated proteins of 32 kD on immunoblots, in addition to the unglycosylated 29-kD form (6,15–18). The sensitivity of the 32-kD bands for cleavage by endoglycosidase H, which specifically removes high-mannose sugar moieties, strongly indicate that these AQP2 forms are ER-retained proteins (15). In contrast, proteins that are properly processed, as is the case for wt-AQP2 in oocytes, the ER retention time is very short and, therefore, only the 29-kD band is detected (Figure 4). The high-mannose glycosylated form of wt-AQP2 (32 kD) is usually only observed when wt-AQP2 is expressed at high levels and with a long exposure time of the film to the blot (*e.g.*, Figure 5).

Cell Biologic Phenotype of Missense AQP2 Mutants Underlying NDI in Families 1 to 4

Except for AQP2-V194I, the AQP2 missense mutants studied here are no exception to the general defect described above. When expressed at a higher level than wt-AQP2 (Figure 4A), which is the result of the injection of higher amounts of mutant AQP2 cRNAs, all mutants conferred reduced water permeability to oocytes (Figure 3) and were partly expressed as high-mannose glycosylated 32-kD proteins (Figure 4, A and B), which is indicative of retention in the ER. As reported before by Goji *et al.* (19), the absence of a 32-kD band in the lane of AQP2-T125M is caused by the loss of the AQP2 N-glycosylation consensus sequence due to the introduced mutation. Additional evidence that all these mutants are retained in the cell is provided by the fact that, compared with wt-AQP2, much less of the AQP2 mutants is expressed in the plasma membranes (Figure 4) and that all these mutants show a dispersed immunocytochemical staining in oocytes (Figure 7).

Besides the 29- and 32-kD bands, a 27-kD AQP2 band was observed, which must be an AQP2 degradation product that misses about 20 amino acids from the N-terminus, because the used antibodies are directed against the AQP2 C-terminus. Although it was seen for all AQP2 mutant proteins and wt-AQP2 (Figures 4A and 5), it was most prominent for AQP2-T125M. This mutant lacks N-linked glycosylation, and the interaction of the sugar moieties of several proteins with the ER molecular chaperones calnexin, calreticulin, and glucosidases I and II has been shown to provide stability (34,35); the presence of relatively high amounts of 27-kD AQP2 in oocytes expressing AQP2-T125M might therefore indicate that N_{123} glycosylation of AQP2 is needed for its stability and further cellular processing. Immunoblots of renal AQP2, however, did not reveal a 27-kD AQP2 band (not shown); it is therefore unclear whether such a product exists and has a function *in vivo*.

In unstimulated polarized MDCK cells, G-AQP2 was mainly expressed in the apical plasma membrane (Figure 8), which is different from the vesicular localization of untagged AQP2 in MDCK cells (29). Although this indicated that the N-terminal GFP interfered with a proper shuttling of AQP2 between vesicles and the apical plasma membrane, the plasma membrane localization also revealed that G-AQP2 was properly folded at the ER and therefore could be used as a control to analyze the distribution pattern of AQP2-T125M in more detail. In contrast to G-AQP2, G-AQP2-T125M showed a dispersed staining pattern in MDCK cells, which was similar to that of G-AQP2–R187C, of which the untagged form is a classical AQP2 mutant in recessive NDI (Figure 8). Such a dispersed expression pattern has also been observed for misfolded and ER-retained mutants of AQP2 and other proteins in different cell types (17,36). Therefore, these results support our data in oocytes that AQP2-T125M is also retained in the ER.

Our data for AQP2-T125M and AQP2-G175R are in contrast to those of Goji *et al.* (19), who used similar techniques but reported that these mutants were only expressed in the plasma membrane and were nonfunctional water channels. According to our results AQP2-T125M is partially functional (Figure 6). The absence of an increased P_f for AQP2-T125M observed by Goji *et al.* might be due to the lower amount of injected cRNAs (3 ng compared with 10 ng in this study). Their immunoblots appear to show a reduced level of expression in plasma membrane compared with total membrane expression for both mutants compared with wt-AQP2, which indicates that both mutants were retained in the cell. In addition, a 32-kD band was visible for AQP2-G175R in total and plasma membranes, but not for wt-AQP2, which also indicates that AQP2-G175R is ER retained in their oocytes. The relatively strong immunocytochemical staining in the plasma membranes of AQP2-T125M and AQP2-G175R reported by Goji *et al.* seems to contradict retention of these mutants in the ER. An explanation for this might be that their AQP2 antibodies are less sensitive for high-mannose glycosylated AQP2 than the antibodies used in our experiments, because (*1*) with ER-retained mutants the plasma membrane contains relatively more 29-kD AQP2 than 32-kD AQP2 compared with the proportions found in intracellular organelles (Figure 4: compare lanes A and B [27]) and (*2*) the AQP2 antibodies used by Goji *et al.* did not detect a 32-kD band or show dispersed immunocytochemical staining for AQP2-T126M, in contrast to what we previously reported (16).

Cell Biologic Basis for NDI in Family 5

Our expression studies in oocytes revealed that the function and routing of AQP2-V194I were similar to those obtained for wt-AQP2, which suggests that the V194I mutation does not result in an AQP2 protein that is involved in NDI. Instead, NDI in family 5 is most likely caused by the splice site mutation (c606+1G>A), which involves a highly conserved nucleotide (37) inherited from the father and the single nucleotide deletion (c652delC) inherited from the mother, because the mutations

are predicted to result in two different truncated proteins that are misfolded and retained in the ER.

Functionality of AQP2 Missense Mutants

High expression levels in oocytes and in CHO cells of three AQP2 mutants (AQP2-T126M, AQP2-A147T, and AQP2-L22V) indicated that they are functional water channels (16,17). The extent of functionality, however, differs between mutants, because at high expression levels, AQP2-A147T was as functional as wt-AQP2 while AQP2-T126M and AQP2-G64R retained 20% of the permeability of wt-AQP2 (27). Similarly it was found in this study that AQP2-L28P, AQP2-V71M, AQP2-G175R, and AQP2-P185A are nonfunctional, whereas AQP2-A47V and AQP2-T125M retained 40 and 25% of the single channel permeability of wt-AQP2, respectively. As has been shown *in vitro*, treatment of cells expressing AQP2-T126M or AQP2-A147T with chemical chaperones facilitated the translocation of these mutants to the plasma membrane (17). Chemical chaperones might be of therapeutic value for the subset of NDI patients with mutant AQP2 proteins that retain a sufficient level of functionality and are retained in the ER.

AQP2 Mutants in Recessive NDI: Reduced Functionality or Just ER Retention?

The *Xenopus* oocyte has a large translational capacity (similar to that of 5×10^4 somatic cells [38]); therefore, high expression levels can be obtained. As is also well known for proteins transiently expressed in mammalian cells, high expression levels lead to a "storage saturation" in the organelle where the protein would only be localized when expressed at low levels, resulting in the appearance of the protein in other organelles. In this study, this feature of organelle overloading was used to determine the water permeability of mutants AQP2 proteins relative to that of wt-AQP2. Thus, we were able to show the presence of high-mannose glycosylated AQP2 in the plasma membrane fraction (Figure 4B). In contrast, endogenously expressed proteins, which are expressed at a level that is manageable for the cell, have never been detected in plasma membranes of cells. Similarly, at moderate expression levels, ER-retained AQP2 mutants do not appear in the plasma membrane of oocytes (28). Furthermore, whereas other ER-retained proteins expressed in mammalian cells *in vitro* or *in vivo* were completely retained in the ER (36,39–43), it has been shown that such ER-retained proteins are often transported to and function in the plasma membrane of oocytes to some extent. For example, the ER-retained but functional cystic fibrosis transmembrane conductance regulator lacking Phe508 (CFTR-ΔF508) confers chloride conductance in oocytes, but it does not exit the ER in mammalian cells (44–47). Similar observations have been made for mutants of the HERG voltage-gated potassium channel that cause hereditary long QT syndrome (43) and mutants of tyrosinase in albinism (36). The high levels of expression of mutant proteins in oocyte plasma membranes has been attributed to a reduced level of degradation, because they appear to be temperature-sensitive and oocytes are cultured at 18°C, whereas mammalian cells are cultured at 37°C (36,43,46). Although it cannot be excluded that reduced water channel function may contribute to NDI, these studies strongly indicate that ER retention and subsequent degradation are the major, and presumably only, reason why missense *AQP2* mutations cause autosomal recessive NDI. This hypothesis is corroborated by the absence of mutant AQP2 proteins in urine of patients with autosomal recessive NDI, whereas AQP2 is easily detected in urine of healthy individuals (48,49). However, only analysis of the expression of such AQP2 mutants in renal principal cells would definitively establish their cellular fate.

In conclusion, we identified seven new *AQP2* mutations and determined the cell-biologic cause of five AQP2 missense mutations identified in patients with autosomal recessive NDI. Our experiments show that the cell-biologic phenotype in oocytes of AQP2 missense mutations in autosomal recessive and dominant NDI is now consistently different, because all 20 AQP2 missense mutations that cause autosomal recessive NDI (6,15,16,50,51) are class II mutations (*i.e.*, leading to misfolding and ER retention). Some of these mutants appear to be able to function as water channels; therefore, the challenge of the future is to find chemical chaperones to treat NDI patients by restoring the routing of partially functional water channels to the plasma membrane.

Acknowledgments

We are indebted to Drs. Heye Arends (Deggendorf, Germany), Ulrike Mau, and Peter Kaiser (Tübingen, Germany) for providing blood samples and to Erhard Klauschenz and John Dickson for sequence analysis of the AQP2 gene in family five. This study was supported by grants from the Dutch Kidney Foundation (C95.5001) and European Community (FMRX-CT97–0128) to PMTD and CHvO, the Dutch Organization for Scientific Research (902-18–292 P), University Medical Center, Nijmegen and European Community (QLK3-CT-2001–00987) to PMTD, the Canadian Institutes of Health Research (MOP-8126) and the Canadian Kidney Foundation to DGB, the Chemischen Industrie and Verbund Klinische Pharmacologie Berlin-Brandenburg to AO and WR, and the Deutsche Forschungsgemeinschaft (MU 1497 2–1) to DM. PMTD is an investigator of the Royal Netherlands Academy of Arts and Sciences, and DGB is a Chercheur de Carrière of Le Fonds de la Recherche en Santé du Québec.

References

1. Deen PMT, Verdijk MAJ, Knoers NVAM, Wieringa B, Monnens LAH, van Os CH, van Oost BA: Requirement of human renal water channel aquaporin-2 for vasopressin-dependent concentration of urine. *Science* 264: 92–95, 1994
2. van Os CH, Deen PMT: Aquaporin-2 water channel mutations causing nephrogenic diabetes insipidus. *Proc Assoc Am Physicians* 110: 395–400, 1998
3. Nielsen S, Chou CL, Marples D, Christensen EI, Kishore BK, Knepper MA: Vasopressin increases water permeability of kidney collecting duct by inducing translocation of aquaporin-CD water channels to plasma membrane. *Proc Natl Acad Sci USA* 92: 1013–1017, 1995
4. Rosenthal W, Seibold A, Antaramian A, Lonergan M, Arthus M-F, Hendy GN, Birnbaumer M, Bichet DG: Molecular identi-

fication of the gene responsible for congenital nephrogenic diabetes insipidus. *Nature* 359: 233–235, 1992
5. Van den Ouweland AM, Dreesen JC, Verdijk MAJ, Knoers NVAM: Mutations in the vasopressin type 2 receptor gene (*AVPR2*) associated with Nephrogenic Diabetes Insipidus. *Nat Genet* 2: 99–102, 1992
6. van Lieburg AF, Verdijk MAJ, Knoers NVAM, van Essen AJ, Proesmans W, Mallmann R, Monnens LAH, van Oost BA, van Os CH, Deen PMT: Patients with autosomal nephrogenic diabetes insipidus homozygous for mutations in the aquaporin 2 water-channel gene. *Am J Hum Genet* 55: 648–652, 1994
7. Mulders SM, Bichet DG, Rijss JPL, Kamsteeg EJ, Arthus MF, Lonergan M, Fujiwara M, Morgan K, Leijendekker R, van der Sluijs P, van Os CH, Deen PMT: An aquaporin-2 water channel mutant which causes autosomal dominant nephrogenic diabetes insipidus is retained in the Golgi complex. *J Clin Invest* 102: 57–66, 1998
8. Kamsteeg EJ, Wormhoudt TA, Rijss JPL, van Os CH, Deen PMT: An impaired routing of wild-type aquaporin-2 after tetramerization with an aquaporin-2 mutant explains dominant nephrogenic diabetes insipidus. *EMBO J* 18: 2394–2400, 1999
9. Kuwahara M, Iwai K, Ooeda T, Igarashi T, Ogawa E, Katsushima Y, Shinbo I, Uchida S, Terada Y, Arthus MF, Lonergan M, Fujiwara TM, Bichet DG, Marumo F, Sasaki S: Three families with autosomal dominant nephrogenic diabetes insipidus caused by aquaporin-2 mutations in the C-terminus. *Am J Hum Genet* 69: 738–748, 2001
10. Marr N, Bichet DG, Lonergan M, Arthus MF, Jeck N, Seyberth HW, Rosenthal W, van Os CH, Oksche A, Deen PM: Heterooligomerization of an Aquaporin-2 mutant with wild-type Aquaporin- 2 and their misrouting to late endosomes/lysosomes explains dominant nephrogenic diabetes insipidus. *Hum Mol Genet* 11: 779–789, 2002
11. Zeitlin PL: Novel pharmacologic therapies for cystic fibrosis. *J Clin Invest* 103: 447–452, 1999
12. Deen PMT, Brown D: Trafficking of native and mutant mammalian MIP proteins. In: *Aquaporins*, edited by Hohmann S, Agre P, Nielsen S, San Diego, CA, Academic Press, 2001, pp 235–276
13. Kuznetsov G, Nigam SK: Folding of secretory and membrane proteins. *N Engl J Med* 339: 1688–1695, 1998
14. Pind S, Riordan JR, Williams DB: Participation of the endoplasmic reticulum chaperone calnexin (p88, IP90) in the biogenesis of the cystic fibrosis transmembrane conductance regulator. *J Biol Chem* 269: 12784–12788, 1994
15. Deen PMT, Croes H, van Aubel RA, Ginsel LA, van Os CH: Water channels encoded by mutant aquaporin-2 genes in nephrogenic diabetes insipidus are impaired in their cellular routing. *J Clin Invest* 95: 2291–2296, 1995
16. Mulders SM, Knoers NVAM, van Lieburg AF, Monnens LAH, Leumann E, Wuhl E, Schober E, Rijss JPL, van Os CH, Deen PMT: New mutations in the AQP2 gene in nephrogenic diabetes insipidus resulting in functional but misrouted water channels. *J Am Soc Nephrol* 8: 242–248, 1997
17. Tamarappoo BK, Verkman AS: Defective aquaporin-2 trafficking in nephrogenic diabetes insipidus and correction by chemical chaperones. *J Clin Invest* 101: 2257–2267, 1998
18. Canfield MC, Tamarappoo BK, Moses AM, Verkman AS, Holtzman EJ: Identification and characterization of aquaporin-2 water channel mutations causing nephrogenic diabetes insipidus with partial vasopressin response. *Hum Mol Genet* 6: 1865–1871, 1997
19. Goji K, Kuwahara M, Gu Y, Matsuo M, Marumo F, Sasaki S: Novel mutations in aquaporin-2 gene in female siblings with nephrogenic diabetes insipidus: Evidence of disrupted water channel function. *J Clin Endocrinol Metab* 83: 3205–3209, 1998
20. Oksche A, Dickson J, Schulein R, Seyberth HW, Muller M: Two novel mutations in the vasopressin V2 receptor gene in patients. *Biochem Biophys Res Commun* 205: 552–557, 1994
21. Bichet DG, Arthus M-F, Lonergan M, Hendy GN, Paradis AJ, Fujiwara TM, Morgan K, Gregory MC, Rosenthal W, Didwania A, et al: X-linked nephrogenic diabetes insipidus mutations in North America and the Hopewell hypothesis. *J Clin Invest* 92: 1262–1268, 1993
22. Kamsteeg EJ, Deen PMT: Detection of aquaporin-2 in the plasma membranes of oocytes: a novel isolation method with improved yield and purity. *Biochem Biophys Res Commun* 282: 683–690, 2001
23. McLean IW, Nakane PK: Periodate-lysine-paraformaldehyde fixative. A new fixation for immunoelectron microscopy. *J Histochem Cytochem* 22: 1077–1083, 1974
24. Richardson JC, Scalera V, Simmons NL: Identification of two strains of MDCK cells which resemble separate nephron tubule segments. *Biochim Biophys Acta* 673: 26–36, 1981
25. Deen PMT, Nielsen S, Bindels RJM, van Os CH: Apical and basolateral expression of Aquaporin-1 in transfected MDCK and LLC-PK cells and functional evaluation of their transcellular osmotic water permeabilities. *Pflugers Arch* 433: 780–787, 1997
26. Deen PMT, van Balkom BW, Savelkoul PJ, Kamsteeg EJ, Van Raak M, Jennings ML, Muth TR, Rajendran V, Caplan MJ: Aquaporin-2: COOH terminus is necessary but not sufficient for routing to the apical membrane. *Am J Physiol Renal Physiol* 282: F330–F340, 2002
27. Marr N, Kamsteeg EJ, Van Raak M, van Os CH, Deen PMT: Functionality of aquaporin-2 missense mutants in recessive nephrogenic diabetes insipidus. *Pflugers Arch* 442: 73–77, 2001
28. Kamsteeg EJ, Deen PMT: Importance of aquaporin-2 expression levels in genotype -phenotype studies in nephrogenic diabetes insipidus. *Am J Physiol Renal Physiol* 279: F778–F784, 2000
29. Deen PMT, Rijss JPL, Mulders SM, Errington RJ, van Baal J, van Os CH: Aquaporin-2 transfection of Madin-Darby canine kidney cells reconstitutes vasopressin-regulated transcellular osmotic water transport. *J Am Soc Nephrol* 8: 1493–1501, 1997
30. Smith BL, Agre P: Erythrocyte Mr 28,000 transmembrane protein exists as a multisubunit oligomer similar to channel proteins. *J Biol Chem* 266: 6407–6415, 1991
31. Verbavatz JM, Brown D, Sabolic I, Valenti G, Ausiello DA, Van Hoek AN, Ma T, Verkman AS: Tetrameric assembly of CHIP28 water channels in liposomes and cell membranes: A freeze-fracture study. *J Cell Biol* 123: 605–618, 1993
32. Baumgarten R, Van De Pol MH, Wetzels JF, van Os CH, Deen PMT: Glycosylation is not essential for vasopressin-dependent routing of aquaporin-2 in transfected Madin-Darby canine kidney cells. *J Am Soc Nephrol* 9: 1553–1559, 1998
33. Kim PS, Arvan P: Endocrinopathies in the family of endoplasmic reticulum (er) storage diseases: Disorders of protein trafficking and the role of er molecular chaperones. *Endocr Rev* 19: 173–202, 1998
34. Gardner TG, Franklin RA, Robinson PJ, Pederson NE, Howe C, Kearse KP: T cell receptor assembly and expression in the absence of calnexin. *Arch Biochem Biophys* 378: 182–189, 2000
35. Kosuge T, Toyoshima S: Increased degradation of newly synthesized interferon-gamma (IFN-gamma) in anti CD3-stimulated

lymphocytes treated with glycoprotein processing inhibitors. *Biol Pharm Bull* 23: 545–548, 2000
36. Halaban R, Svedine S, Cheng E, Smicun Y, Aron R, Hebert DN: Endoplasmic reticulum retention is a common defect associated with tyrosinase-negative albinism. *Proc Natl Acad Sci USA* 97: 5889–5894, 2000
37. Rogan PK, Faux BM, Schneider TD: Information analysis of human splice site mutations [published erratum appears in *Hum Mutat* 13: 82, 1999]. *Hum Mutat* 12: 153–171, 1998
38. Roeder RG: Multiple forms of deoxyribonucleic acid-dependent ribonucleic acid polymerase in Xenopus laevis. Levels of activity during oocyte and embryonic development. *J Biol Chem* 249: 249–256, 1974
39. Pathak RK, Merkle RK, Cummings RD, Goldstein JL, Brown MS, Anderson RG: Immunocytochemical localization of mutant low density lipoprotein receptors that fail to reach the Golgi complex. *J Cell Biol* 106: 1831–1841, 1988
40. Lloyd ML, Olsen WA: A study of the molecular pathology of sucrase-isomaltase deficiency. A defect in the intracellular processing of the enzyme. *N Engl J Med* 316: 438–442, 1987
41. Waheed A, Parkkila S, Zhou XY, Tomatsu S, Tsuchihashi Z, Feder JN, Schatzman RC, Britton RS, Bacon BR, Sly WS: Hereditary hemochromatosis: Effects of C282Y and H63D mutations on association with beta(2)-microglobulin, intracellular processing, and cell surface expression of the HFE protein in COS- 7 cells. *Proc Natl Acad Sci USA* 94: 12384–12389, 1997
42. Hory B, Roussanne MC, Drueke TB, Bourdeau A: The calcium receptor in health and disease. *Exp Nephrol* 6: 171–179, 1998
43. Ficker E, Thomas D, Viswanathan PC, Dennis AT, Priori SG, Napolitano C, Memmi M, Wible BA, Kaufman ES, Iyengar S, Schwartz PJ, Rudy Y, Brown AM: Novel characteristics of a misprocessed mutant HERG channel linked to hereditary long QT syndrome. *Am J Physiol Heart Circ Physiol* 279: H1748–H1756, 2000
44. Drumm ML, Wilkinson DJ, Smit LS, Worrell RT, Strong TV, Frizzell RA, Dawson DC, Collins FS: Chloride conductance expressed by delta F508 and other mutant CFTRs in Xenopus oocytes. *Science* 254: 1797–1799, 1991
45. Makhina EN, Nichols CG: Independent trafficking of KATP channel subunits to the plasma membrane. *J Biol Chem* 273: 3369–3374, 1998
46. Denning GM, Anderson MP, Amara JF, Marshall J, Smith AE, Welsh MJ: Processing of mutant cystic fibrosis transmembrane conductance regulator is temperature-sensitive. *Nature* 358: 761–764, 1992
47. Cheng SH, Gregory RJ, Marshall J, Paul S, Souza DW, White GA: Defective intracellular transport and processing of CFTR is the molecular basis of most cystic fibrosis. *Cell* 63: 827–834, 1990
48. Deen PMT, van Aubel RA, van Lieburg AF, van Os CH: Urinary content of aquaporin 1 and 2 in nephrogenic diabetes insipidus. *J Am Soc Nephrol* 7: 836–841, 1996
49. Kanno K, Sasaki S, Hirata Y, Ishikawa S, Fushimi K, Nakanishi S, Bichet DG, Marumo F: Urinary excretion of aquaporin-2 in patients with diabetes insipidus. *N Engl J Med* 332: 1540–1545, 1995
50. Tamarappoo BK, Yang B, Verkman AS: Misfolding of mutant aquaporin-2 water channels in nephrogenic diabetes insipidus [In Process Citation]. *J Biol Chem* 274: 34825–34831, 1999
51. Canfield M, Tamarappoo BK, Moses AM, Verkman AS, Holtzman EJ: Novel AQP2 mutations as a cause of partially dDAVP-responsive post V2 receptor congenital nephrogenic diabetes insipidus (CNDI). *J Am Soc Nephrol* 7: 1611, 1996
52. LeBlanc Straceski JM, Montgomery KT, Kissel H, Murtaugh L, Tsai P, Ward DC, Krauter KS, Kucherlapati R: Twenty-one polymorphic markers from human chromosome 12 for integration of genetic and physical maps. *Genomics* 19: 341–349, 1994